Local learning rules: Predicted influence of dendritic location on synaptic modification in spike-timing-dependent plasticity

Ausra Saudargiene[1,2], Bernd Porr[1] and Florentin Wörgötter[1]

[1]Department of Psychology, University of Stirling, Stirling FK9 4LA, Scotland
[2]Department of Informatics, Vytautas Magnus University, Kaunas, Lithuania

Correspondence:
Florentin Wörgötter
Department of Psychology
University of Stirling
Stirling
FK9 4LA
UK
Phone: +44 (0)1786 466369
FAX: +44 (0)1786 467641
Email: worgott@cn.stir.ac.uk

Abstract

Recent indirect experimental evidence suggests that synaptic plasticity changes along the dendrites of a neuron. Here we present a synaptic plasticity rule which is controlled by the properties of the pre- and post-synaptic signals. Using recorded membrane traces of back-propagating and dendritic spikes we demonstrate that LTP and LTD will depend specifically on the shape of the post-synaptic depolarization at a given dendritic site. We find that asymmetrical spike-timing dependent plasticity (STDP) can be replaced by temporally symmetrical plasticity within physiologically relevant time-windows if the post-synaptic depolarization rises shallow. Pre-synaptically the rule depends on the NMDA channel characteristic and the model predicts that an increase in Mg^{2+} will attenuate the STDP curve without changing its shape. Furthermore, the model suggests that the profile of LTD should be governed by the post-synaptic signal while that of LTP mainly depends on the pre-synaptic signal shape.

1 Introduction

The electrical properties of dendrites vary depending on cell-type, dendritic location as well as on the state of developmental maturation of a neuron (Stuart and Spruston, 1998; Golding et al., 1999; Schiller et al., 2000; Williams et al., 1993; Monyer et al., 1994). In addition, dendritic compartments are often to a large degree decoupled from each other such that local, site-specific interactions can take place in independence making each single dendrite functionally similar to a whole computational network (Mel, 1994; Poirazi et al., 2003). As a consequence it is by now widely accepted that the different parts of a neuronal dendrite may serve different computational purposes. Recent experimental evidence implies that this feature does not only apply to the moment-to-moment computations taking place at a neuron but in a similar, site-specific way also to synaptic plasticity (Froemke and Dan, 2003). This is suggested by the fact that the electrical and chemical signals which drive synaptic change can be very different at different sites (Häusser and Mel, 2003; Golding et al., 2002).

Two types of long-lasting synaptic changes are in general observed, long term potentiation (LTP) and long term depression (LTD) (Bliss and Lomo, 1970; Bliss and Gardner-Edwin, 1973; Bliss and Lomo, 1973). More recently it has been found that synaptic weights can grow and shrink at the same synapse depending on the temporal order of the pre-synaptic and the post-synaptic signal: If the pre-synaptic signal occurs before the post-synaptic signal (denoted by $T > 0$), weights will grow, while they will shrink if the temporal order is reversed ($T < 0$, called spike-timing dependent plasticity, STDP (Magee and Johnston, 1997; Markram et al., 1997). To induce STDP a strong depolarization is necessary presumably for the unblocking of NMDA-channels (Debanne et al., 1998; Chen et al., 1999; Nishiyama et al., 2000; Sjöström et al., 2001; Kovalchuk et al., 2000; Bi, 2002). Close to the soma such a depolarization is achieved by back-propagating (BP) somatic action potentials, which become longer in duration and smaller in amplitude while propagating into the dendritic tree (Magee and Johnston, 1997; Linden, 1999). In distal dendritic parts, where BP spikes are highly attenuated (Stuart and Spruston, 1998; Häusser and Mel, 2003) synaptic plasticity may be triggered by local dendritic Na^{+}- and Ca^{2+} channel dependent spikes (Golding et al., 2002; Larkum et al., 2001), which are initiated by strong cooperative synaptic inputs and/or BP spikes.

The effects discussed above indicate that the different shapes of BP- and dendritic-spikes, which change along the dendrite, should lead to different post-synaptic influences on plasticity depending on the dendritic site. This study sets out to test this hypothesis by means of a model. Based on the assumption that differential Hebbian learning rules (Sutton and Barto, 1981; Kosco, 1986; Klopf, 1986; Porr and Wörgötter, 2003) can capture STDP (Roberts, 1999; Xie and Seung, 2000; Wörgötter and Porr, 2004), we will develop an analytically treatable rule. This rule uses the membrane potential of the post-synaptic cell as the only variable control parameter. Several predictions arise from this model which should be experimentally testable. Such local, site-specific plasticity may be important because at a single neuron different rules for synaptic plasticity can coexist this way. Networks, which can implement such "local learning properties", will certainly demonstrate substantially enriched computational properties.

Numerical results from a simpler model are published in Saudargiene et al. (2004).

2 The Model

Conventionally, low Ca^{2+} concentration is associated to LTD and high to LTP (Hansel et al., 1997; Yang et al., 1999). A purely concentration dependent plasticity rule, however, creates a problem. Several authors have discussed that, as a consequence of a purely concentration dependent plasticity rule, a second LTD window should exist for long temporal intervals between pre- and post-synaptic activity (Bi, 2002; Karmarkar and Buonomano, 2002; Shouval et al., 2002; Abarbanel et al., 2003). Only one study seems to support this so far (Nishiyama et al., 2000). Thus, we propose to use a rule that is gradient dependent instead (Bi, 2002). This rule will model in an abstract way both, increase and decrease, of the Calcium concentration through gating and elimination which follows a sequence of pre- and post-synaptic activity. The goal is to arrive at a closed form description of both processes in order to keep the rule analytically treatable.

To this end, it is necessary to analyse the different processes that happen during a pre- and a post-synaptic event to some degree first.

It is generally accepted that NMDA channels are instrumental for the induction of LTP (Malenka and Nicoll, 1999) but they seem to be also involved in LTD in many cases (Kombian and Malenka, 1994; Sawtell et al., 1999; Hrabetova et al., 2000; Kourrich and Chapman, 2003). Accordingly, it seems that it is mainly that part of the Calcium that enters through NMDA channels which is involved in inducing plasticity. Alternative hypotheses for the generation of STDP shall be discussed below. For the model we will thus assume that pre-synaptically, or rather at the membrane of the post-synaptic cell, the time course of NMDA-channel opening and the Calcium flux through these channels is crucial. To simulate this we use the textbook definition of an NMDA channel function as usual (Jahr and Stevens, 1990; Koch, 1999):

$$g_N(t) \;=\; \hat{g}\; c_N \;=\; \hat{g}\; \frac{e^{-b_1 t} - e^{-a_1 t}}{1 + \kappa e^{-\gamma V_m(t)}} \tag{1}$$

For simpler notation, in general we use inverse time-constants $a_1 = \tau_a^{-1}$, $b_1 = \tau_b^{-1}$. Parameters were: the peak conductance $\hat{g} = 4\ nS$, $a_1 = 3.0/ms$,$b_1 = 0.025/ms$, $\gamma = 0.06/mV$. Since we will not vary the Mg^{2+} concentration we have already abbreviated: $\kappa = \eta[Mg^{2+}]$, $\eta = 0.33/mM$, $[Mg^{2+}] = 1\ mM$.

In our formalism we only need the *normalized* conductance function c_N, which represents the temporal channel characteristics. This time-course of the NMDA-channel opening can mainly be associated with pre-synaptic influences taking place at the cell-membrane (Kampa and Stuart, 2003a).

Post-synaptically the model must capture the transient nature of the Calcium concentration changes. In our model we assume that Calcium influx but also Calcium elimination depend directly (influx) or indirectly (elimination) on the post-synaptic membrane potential[1]. This allows us to design a closed form approximation of the relevant post-synaptic processed which keeps the model analytic. To this end we use the derivative of the membrane potential V_m, which creates the required bi-phasic time course (positive part: influx, negative part: elimination) after a BP- or a dendritic spike. To capture the prolonged time courses of the Calcium gradients (Koester and Sakmann, 1998; Wessel et al., 1999; Koester and Sakmann, 2000; Sabatini et al., 2002), we filter the derivative with an appropriate (non-standard) low-pass filter h, designed to emulate the time course of Calcium influx. (There is currently no quantitative data on the time course of the elimination.) Thus, as the post-synaptic influence we use:

$$F(t) = \frac{d[V_m(t) * h(t)]}{dt} \tag{2}$$

where $h(t)$ is the mentioned low-pass filter with which V_m is convolved (denoted by the asterisk). The same filter has been used throughout this study:

$$h(t) = \sigma\ (e^{-b_h t} - e^{-a_h t}), \tag{3}$$

with parameters: $a_h = 1/1ms$, $b_h = 1/40ms$. The shape of this special filter models the steep rise but long tail of the observed Calcium transients

[1]For influx this assumption is straight-forward. For elimination one should consider that this process is mainly driven by Calcium itself, hence it follows from the strength of the preceding influx

(Koester and Sakmann, 1998; Wessel et al., 1999; Koester and Sakmann, 2000; Sabatini et al., 2002).

The correlative nature of pre- and post-synaptic events is captured as usual by a correlation integral which defines our plasticity rule after one pulse pairing T:

$$\Delta\rho(T) = \mu \int_0^\infty c_N(t,T)\; F(t,T)dt \tag{4}$$

where ρ is the synaptic weight. Note, this is a causal correlation, where the dependence on T is spelt out in Eq. 14,15 in the Appendix.

Note that this formalism in a physiological situation is only dependent on the membrane potential, which is, thus, the only free control parameter in our model. In an experiment, the Magnesium concentration can also be varied and we will discuss this below.

The remainder of this article is structured as follows. In the next section we will calculate the integral (Eq 4). Readers not interested in the details of the mathematical solution may want to skip this part. The section that follows will discuss the properties of the obtained solution. In spite of their complicated looking structure (which comes mainly from a nasty mix of coefficients) several interesting results can be extracted. Most notably three observation will be derived: 1) We will demonstrate that differential Hebbian plasticity with conventionally shaped STDP curves (LTD and LTP) can turn into a more symmetrical, plain Hebbian plasticity dominated by LTP as a function of the post-synaptic depolarization. 2) Furthermore, we will show how plasticity gets attenuated by increasing the concentration of Mg^{2+}. 3) Finally the solution predicts that the LTP part of STDP should be dominated mainly by the NMDA-characteristic, while the LTD part should be governed by the post-synaptic potential. We will then use a numerical fit of real membrane potential traces recorded at different locations of a dendriteto show how plasticity would change in a site-dependent way. Finally we will discuss our results.

A rule similar to this, but without the low-pass filter, was investigated by Saudargiene et al. (2004) without obtaining an analytical solution, with artificial input signals only and without assessing the influence of the Magnesium.

3 Results

3.1 Solution

We define:

$$V_m(t) * h(t) = \varphi \cdot t^\beta \left(e^{-b_2 t} - e^{-a_2 t}\right), \tag{5}$$

with $\beta = 0, 1, 2 \ldots$. This way we have absorbed the filtering process into a closed form description. This is permitted, because convolving with a filter and taking a derivative when computing F (Eq 2) are commutative.

The function $V_m(t) * h(t)$ takes the shape of an temporally prolonged alpha-function, where $\tau_r = 1/a_2$ determines the rising and $\tau_f = 1/b_2$ the falling flank. Note, we need $\tau_f > \tau_r$ to get an alpha-function shape. Its amplitude can be adjusted by the constant φ. The parameter β allows generating convex (e.g., $\beta \geq 2$) or concave ($\beta = 0$) initial rising shapes. Specific parameters for Eq. 5 were determined by fitting the numerically obtained traces of F (see e.g. Fig. 4).

We need to calculate the integral Eq. 4. This is done in the Laplace domain, because causal correlations can be more easily treated there as compared to the time domain. We find for F:

$$F(s) = \varphi \cdot \left(\frac{s \cdot \beta!}{(s + b_2)^{\beta+1}} - \frac{s \cdot \beta!}{(s + a_2)^{\beta+1}}\right) \tag{6}$$

The dependence of the NMDA channel function on the membrane potential can be approximated using a Taylor expansion around $V_m = 0\ mV$.

$$c_N(t) = (e^{-b_1 t} - e^{-a_1 t}) \cdot \left(\frac{1}{\kappa + 1} + \frac{\gamma \kappa V_m(t)}{(\kappa + 1)^2} + \ldots\right) \tag{7}$$

We will now only take the part of the Taylor expansion which is not dependent on V_m (first term) and use its Laplace transform:

$$c_N(s) \approx \frac{1}{\kappa + 1} \left(\frac{a_1 - b_1}{(s + a_1)(s + b_1)}\right) \tag{8}$$

This gives us an error of $\approx 0.75\%/mV$. Note the error is zero at $V_m = 0$, when most of the NMDA channels are open. Thus, this approximation becomes the true solution for the steady state $V_m = 0$, which justifies this procedure.

The integral Eq. 4 is in the Laplace domain given by:

$$\Delta\rho = \mu \frac{1}{2\pi} \int_{-\infty}^{+\infty} c_N(-\imath\omega) e^{-\imath\omega T} F(\imath\omega) d\omega \tag{9}$$

where $e^{-\imath\omega T}$ is the temporal shift operator. This equation can be solved by Plancherel's theorem using the methods of residuals for all different values of β. Solutions are plotted for $\beta = 0$ and $\beta = 2$ in Fig. 1 B,D.

Below we present the resulting terms for $\beta = 0$ and $\beta = 2$.

3.1.1 Case: $\beta = 0$, concave growing spike shapes

Absorbing φ into μ, we find for $T \geq 0$:

$$\begin{aligned} \Delta\rho = \frac{\mu}{\kappa+1} \quad & \Big[\Big(\tfrac{1}{(b_1+b_2)} - \tfrac{1}{(b_1+a_2)}\Big) b_1 \; e^{-b_1 T} \\ & - \Big(\tfrac{1}{(a_1+b_2)} - \tfrac{1}{(a_1+a_2)}\Big) a_1 \; e^{-a_1 T}\Big] \end{aligned} \tag{10}$$

and for $T < 0$:

$$\Delta\rho = \frac{\mu(a_1 - b_1)}{\kappa+1}\left[\frac{b_2 e^{b_2 T}}{(b_2+a_1)(b_2+b_1)} - \frac{a_2 e^{a_2 T}}{(a_2+a_1)(a_2+b_1)}\right] \tag{11}$$

3.1.2 Case: $\beta = 2$, convex growing spike shapes

For $T \geq 0$:

$$\begin{aligned} \Delta\rho = \frac{\mu}{\kappa+1} \quad & \Big[\Big(\tfrac{2b_1}{(b_1+b_2)^3} - \tfrac{2b_1}{(b_1+a_2)^3}\Big) e^{-b_1 T} \\ & - \Big(\tfrac{2a_1}{(a_1+b_2)^3} - \tfrac{2a_1}{(a_1+a_2)^3}\Big) e^{-a_1 T}\Big] \end{aligned} \tag{12}$$

and for $T < 0$:

$$\begin{aligned} \Delta\rho = \frac{\mu(a_1 - b_1)}{\kappa+1} \quad & \Big[\Big(\tfrac{a_2(b_1^2+2b_1a_2+a_2^2)(a_1^2+2a_1a_2+a_2^2)T^2}{(a_1+a_2)^3(b_1+a_2)^3} \\ & + \tfrac{2(b_1+a_2)(a_1b_1-a_2^2)(a_1+a_2)T}{(a_1+a_2)^3(b_1+a_2)^3} \\ & - \tfrac{2(a_1^2b_1+a_1b_1(b_1+3a_2)-a_2^3)}{(a_1+a_2)^3(b_1+a_2)^3}\Big) e^{a_2 T} \\ & - \Big(\tfrac{b_2(b_1^2+2b_1b_2+b_2^2)(a_1^2+2a_1b_2+b_2^2)T^2}{(a_1+b_2)^3(b_1+b_2)^3} \\ & + \tfrac{2(b_1+b_2)(a_1b_1-b_2^2)(a_1+b_2)T}{(a_1+b_2)^3(b_1+b_2)^3} \\ & - \tfrac{2(a_1^2b_1+a_1b_1(b_1+3b_2)-b_2^3)}{(a_1+b_2)^3(b_1+b_2)^3}\Big) e^{b_2 T}\Big] \end{aligned} \tag{13}$$

These results show that V_m, which determines the shape of the post-synaptic potential also determines the characteristics of plasticity as discussed with a different rule by Rao and Sejnowski (2001).

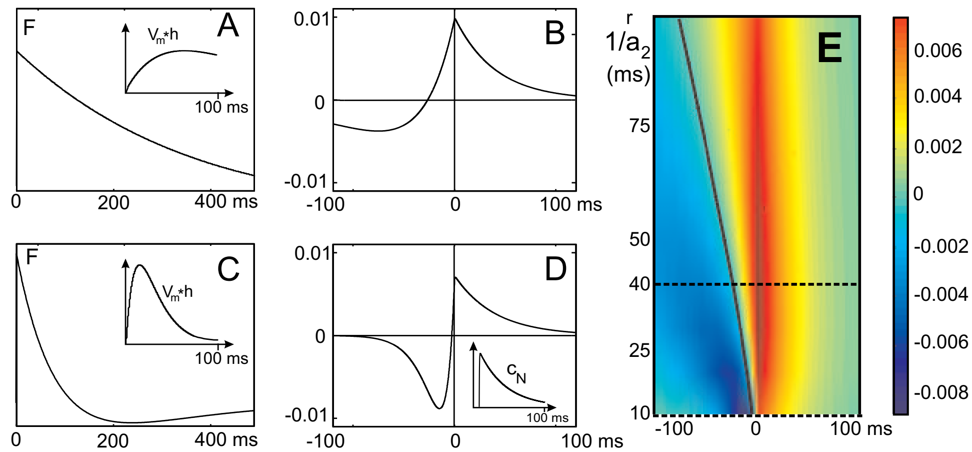

Figure 1: Analytically calculated functions F **(A,C)** and the resulting STDP curves **(B,D)**. **A,C)** F is calculated using Eqs. 2,5. Insets in A,C show the functions $V_m \star h$ (Eq. 5) at a magnified time scale, which matches that in panels **B,D**. Parameters: **(A)** $\beta = 0$, $a_2 = 1/10ms$, $b_2 = 1/15ms$, $\varphi = 0.2$; **(C)** $\beta = 0$, $a_2 = 1/40ms$, $b_2 = 1/60ms$, $\varphi = 0.2$. **B,D)** STDP curves calculated analytically using Eqs. 10, 11. The inset in D shows the temporal characteristics of the NMDA channel function c_N. **E)** Analytically calculated STDP curves as a function of the shape of F. Parameter a_2 in Eqs. 10, 11 varied from $1/100ms$ to $1/10ms$, $b_2 = 0.666a_2$, $\beta = 0$. Solid line indicates the zero crossing. Dotted lines at $\tau_r = 1/a_2 = 40ms$ and $10ms$ correspond to the cases presented in A, B and C, D, respectively. A differential Hebbian plasticity characteristics turns into Hebbian-type plasticity when the depolarization has a slow rising phase (decreased a_2 in Eq. 5).

3.2 Properties of the Solution

3.2.1 Influence of the membrane potential

One interesting aspect of this formalism is revealed when looking at the zero-crossing where the LTP part (positive) is separated from the LTD part (negative). The zero crossing shifts towards negative values of T with increasingly shallow rising flanks of the post-synaptic signal. The color panel in Fig. 1 demonstrates how the analytical solutions develop for different shapes of V_m. The solid line depicts their zero crossing. This shows that a differential Hebbian characteristic, where the STDP curves contain an LTD and an LTP part, turns more and more into a Hebbian characteristic (only LTP), when the time constant $\tau_r = 1/a_2$ from V_m gets larger. This, however, is the case for a prolonged, slowly rising depolarization as shown by the membrane potentials in Fig. 1 A,B. The top two panels (A,B) correspond to a time-constant $\tau_r = 1/a_2$ of 40 ms; the bottom ones (C,D) to 10 ms. The second time-constant $\tau_f = 1/b_2$ was always adjusted to $1.5\tau_r$.

In an experimental situation the exact point in time of a post-synaptic spike cannot be determined at the location of the synapse. Thus, values of T can only be given relative to the time-point of the stimulation pulse or relative to the crossing of a threshold by the elicited spike. This will shift the STDP curves but will leave the above discussed effects unaffected.

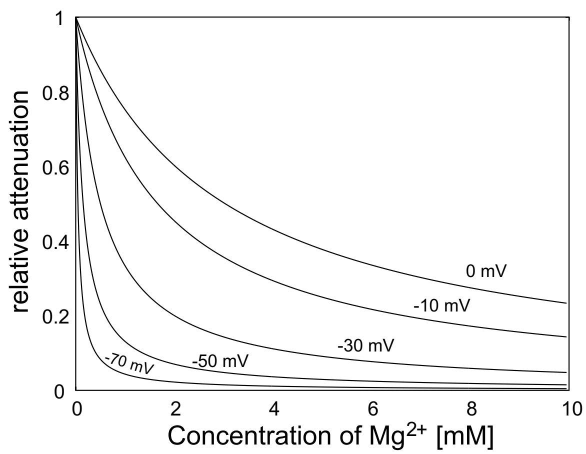

Figure 2: Influence of the Magnesium concentration on the amplitude of the STDP curve. Curves for different depolarization levels are shown.

3.2.2 Influence of the Magnesium concentration

Fig. 2 shows how the Magnesium concentration will attenuate plasticity at different levels of the post-synaptic membrane potential. First we observe from Eq. 10-13, that these attenuation characteristics should only affect the amplitude of an STDP curve leaving its shape as it is (in contrast to the prediction from the model by Abarbanel et al. (2003)). Even when we take the full model (going beyond the first term of the Taylor series) this assumtions still essentially holds, because, depending on V_m, the contriutions of the higher order terms are one or two orders of magnitude less than that of the first order term. The top curve assumes a post-synaptic depolarization to the zero millivolt level and follows the hyperbolic function $\frac{1}{1+\kappa}$. If depolarization is less, attenuation will be stronger, and the hyperbolic characteristic will turn more and more into that of a sharply decaying exponential $\frac{1}{1+\kappa e^{-\gamma V_m}}$, shown by the other curves. Even for the strongest depolarization, we observe that more than 60% attenuation is to be expected at a concentration of 5 mM Magnesium. To measure these curves it would be required to vary $[Mg^{2+}]$ and to generate a controlled, rather rectangular post-synaptic depolarization to the desired level. This should be possible when studying STDP at a synapse close to the soma, where low-pass filtering due to the space and time constants of the membrane would be still limited.

A strong deviation from the functional characteristics shown in Fig. 2 would indicate that also other than NMDA-dependent influences are important. This test is especially interesting for the LTD part of the STDP curves where mechanisms that involve voltage gated Calcium channels and mGlu receptors have been suggested (Oliet et al., 1997; Normann et al., 2000).

3.2.3 Split of Terms

As a third observation we find that the last four equations (Eq. 10-13) exhibit a *split of terms*. This can be seen by looking at the exponential functions in Eq. 10,12 valid for $T > 0$, which only depend on constants a_1 and b_1, which came from the NMDA channel function. On the other hand the exponential functions in Eq. 11,13, which are responsible for $T < 0$, depend on a_2 and b_2, which came from F.

This property is interesting and slightly paradoxical. First we note that Eq. 4 is given as closed form for all positive and negative values of T. In spite of this, the solution splits at $T = 0$ in a negative part which covers LTD and a positive part for LTP. Such a property is indeed required, because from biophysically studies it is known that the mechanisms which lead to LTP and LTD are substantially different (Bi, 2002; Lisman, 1994; Otmakhov et al., 1997). Hence both sides of an STDP curve really represent two distinctively different conditions arguing for two different coincidence detector mechanisms (Karmarkar and Buonomano, 2002). This requirement, however, is captured in a natural way by our formalism because of the mathematical properties of the correlation integral. This leads to a split of the curve at $T = 0$ where the LTD part of the curve turns to the LTP part. Thus, we note that the right parts of the curves in Fig. 1 B,D are very similar to the time course of the NMDA channel function (compare to inset in D). Looking

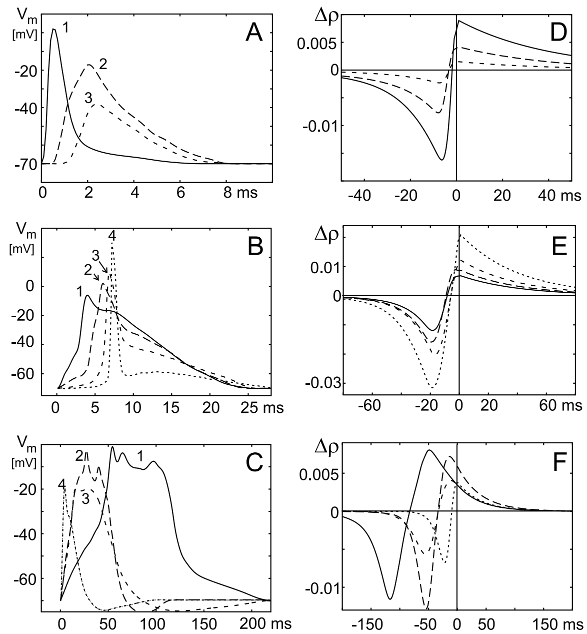

Figure 3: Depolarising potentials ; **(A)** BP-spikes and **(B,C)** dendritic spikes adopted from Larkum et al. (2001) and the resulting STDP curves **(D-E)**. **A)** Back-propagating spikes, measured at different distances from the soma (1: $170\mu m$, 2: $420\mu m$, 3: $630\mu m$). **B)** Forward-propagating dendritic spikes, measured 1: $700\mu m$, 2: $500\mu m$, 3: $250\mu m$ from the soma and at the soma (4). Spikes were elicited by current injection at $700\mu m$ from the soma; **C)** Dendritic spikes, measured $860\mu m$ from the soma. Current injections of the different duration with peak times of 1: $50ms$, 2: $10ms$, 3: $5ms$, 4: $2ms$ were made at $930\mu m$ from the soma to elicit these spikes. **D-F)** Numerically calculated STDP curves. The recorded membrane potentials were filtered with the filter h and the derivatives of the resulting signals were determined to arrive at F. Filter parameters as in Eq. 3. Scale factors σ to maintain amplitude relations between the different spikes were set to: **D)** curves 1-3 in A: $\sigma = 0.1021, 0.0381, 0.0416$; **E)** curves 1-4 in B: $\sigma = 0.0131, 0.0173, 0.0256, 0.0610$; **F)** curves 1-4 in C: $\sigma = 0.0126, 0.0136, 0.0120, 0.0213$. The obtained trace F and the NMDA channel function c_N (Eq. 1) were substituted in Eqs. 14,15 to calculate the STDP curves.

at the insets in Fig. 1 A,D, plotted with a magnified time scale, one finds that the left part of the STDP curves corresponds to the mirror image of the function $V_m * h$ (of which F is the derivative).

Hence we conclude that the LTP part of STDP should in the first instance be dominated mainly by the NMDA-characteristic, while the LTD part should be governed by the post-synaptic potential. Only when considering higher order terms from the Taylor expansion in Eq. 9, mixed terms are found, too, in the final results. The error estimation given in conjunction with Eq. 9, however, shows that their influence may remain limited.

Note, this property is not directly coupled to the functions which determine the plasticity rule as such. Instead it derives from the properties of causal correlation. Thus, a split of terms should always be observed even if the functions F and c_N should have to be replaced by other more complex terms in a more advanced version of this model.

3.3 Numerical results using real potential traces

The left panels in Fig. 3 adopted from Larkum et al. (2001) show how the shapes of BP-spikes and dendritic spikes change with distance from the soma. The right panels display the corresponding STDP weight change curves calculated numerically with the plasticity rule introduced above. Specific details concerning the way to calculate the numerical results are given in the Appendix.

In general we observe that the asymmetrical characteristic of the STDP curve is reproduced in all cases. The left part of the curve, representing LTD, is more pronounced than the right part, which also corresponds to physiological observations (Debanne et al., 1998; Bi and Poo, 2001; Feldmann, 2000). Amplitude differences in the STDP curves correspond to amplitude differences of the membrane potential signals. Within the limitations of our state variable model, this may reflect the fact that weaker membrane potential changes will probably also lead to a less pronounced plasticity (Golding et al., 2002). As expected from the analytical results, we observe that the STDP curves that belong to broader, temporally prolonged membrane potentials are shifted to the left as compared to those which arise from sharp, short spikes. This effect arises from the slope of the rising flank of the spike and not from its temporal duration. Thus, the dendritic location should have a major influence on the shape of synaptic plasticity, because it determines the shape of the membrane potential following a BP- or dendritic spike.

The effect that shallow slopes lead to negative zero-crossings in the STDP

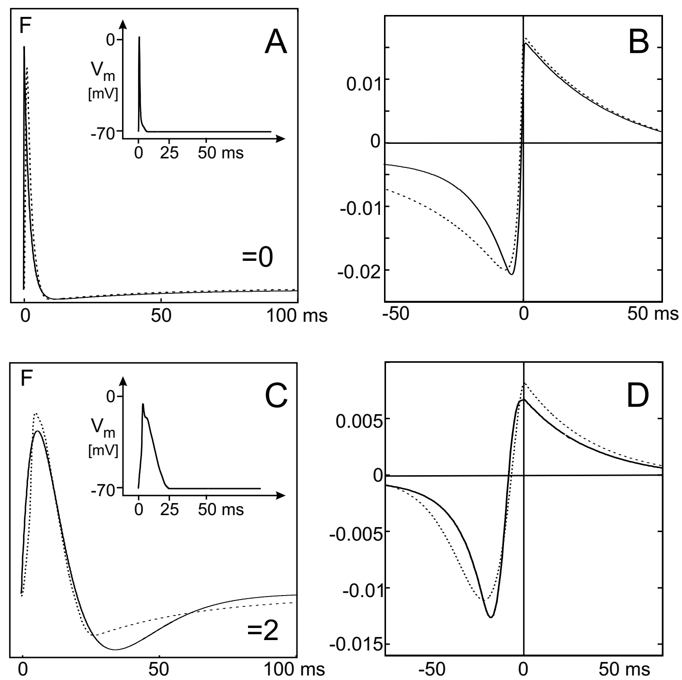

Figure 4: Comparison between numerical and analytical results. **A,C)** Function F derived from the measured membrane potentials (solid) and their analytical fits (dotted). Insets in **(A,C)** show the corresponding BP-spike, measured $170\mu m$ from the soma (**A**), and the forward-propagating dendritic spike (**C**), measured at the soma. Adopted from Larkum et al. (2001). **B,D)** Numerical and analytical STDP curves. Results are shown for a short steep BP-spike **(A,B)** and a prolonged dendritic spike **(C,D)**. Curve fitting: The recorded membrane potentials were filtered with the filter h (Eq. 3; **A:** $\sigma = 0.1021$, **B:** $\sigma = 0.0126$) and derivatives taken to yield F. These curves were fitted with the analytical form of F (Eqs. 2,5). Parameters were: **A)** $\beta = 0$, $a_2 = 1/2ms$, $b_2 = 1/38.5ms$, $\varphi = 0.089$; **C)** $\beta = 2$, $a_2 = 1/0.1ms$, $b_2 = 1/10ms$, $\varphi = 118.222$. **B,D)** STDP curves calculated numerically (solid) using Eqs. 14,15 and analytically (dotted) using Eqs. 10-13 with the same parameters as in **A,C**. Note in **A,B** we use $\beta = 0$ and in **C,D** $\beta = 2$.

curves can be seen best in panels C and F of Fig. 3. The steepest dendritic spike leads to an STDP curve with a zero-crossing very close to the origin, while spikes with more shallow-rising flanks lead to leftward shifted curves.

A similar leftward shift of the STDP curve has been observed recently by Kampa and Stuart (2003b) using triplets of weak post-synaptic potentials to elicit plasticity. These studies suggest that this leads either to a delayed dendritic spike, which will shift the STDP curve as discussed above, or a slowly rising dendritic spike. In both cases their findings can be directly related to the effects observed here.

Fig. 4 shows how analytical and numerical results compare for one BP- (A,B) and one dendritic spike (C,D). The left panels show the original signals (insets), and the functions F, numerically calculated from the spikes (solid lines) or fitted by means of the analytical function for F given in Eq. 2,5 (dotted lines). Numerical and analytical STDP curves are shown to the right. The LTD part of the analytical curves is slightly bigger, but otherwise numerical and analytical curves match nicely. Such excellent fits cannot be obtained for all individual BP- or dendritic spikes, because they are often noisier and less smooth (e.g. Fig. 3 B,C). If one considers average potentials, however, the necessary smoothness is re-obtained. Signal averaging would essentially capture the situation that most physiological experiments use multiple pulse-pairings to induce plasticity.

4 Discussion

In this study we have introduced a gradient dependent synaptic plasticity rule similar to rules discussed in the context of differential Hebbian learning. The goal was to test the idea of site-specific plasticity. The model makes three testable predictions:

1. The shape of the post-synaptic membrane potential should play a major role in determining the actual characteristic of STDP. More specifically the results suggest that synaptic plasticity in the central window of $T\pm \approx 50\ ms$ can change from STDP to LTP if the membrane potential rises slowly. This effect could be measured at synapses close to the soma by controlled post-synaptic depolarization while blocking the spike. Different rising phases of the depolarization should lead to a curve for the zero-crossing similar to that in Fig. 1 E.

2. A change in the Magnesium concentration should only affect the amplitude but not the shape of STDP. This effect could be measured by applying different concentrations of Mg^{2+} to the slice. A curve should be obtained similar to those shown in Fig. 2.

3. Finally the model suggests that during STDP the profile of LTD should be governed by the characteristic of the post-synaptic signals while that of LTP mainly depends on the pre-synaptic signal shape. Physiologically this is supported by results that the order of the pre- and post-synaptic signals does indeed directly lead to an asymmetry of the triggered second messenger processes (Bi, 2002; Lisman, 1994; Otmakhov et al., 1997). This effect, which originates from the "split of terms", can be tested by by manipulating either the response properties of the NMDA channel (e.g. pharmacologically using APV) or the *shape* of the post-synaptic membrane depolarization (e.g. using specific depolarization pulses while blocking the spike). The first type of manipulations should mainly affect the shape of the LTP part of the curve, while the second would change mainly the LTD characteristic.

4.1 Motivation

The notion that site specific plasticity can exist in real neural networks is currently indirectly supported by findings that show that the membrane properties of real neurons strongly change along its dendrites (Häusser et al., 2000). In addition, different timing properties have been reported at proximal and distal regions of apical dendrites in layer 2/3 pyramidal cells for eliciting STDP (Froemke and Dan, 2003). This has been interpreted as a spatial effect possibly influencing synaptic development (Froemke and Dan, 2003). Site-specific plasticity would make individual neurons much more flexible in their computational properties, because different rules would exist at the same neuron, ideally controlled by means of only one parameter (here V_m).

Apart from the biological consequences, this property should also be of direct relevance also to artificial neural network design. With such rules local network learning can be implemented and ANNs can be sub-structured. This, however, makes it necessary to design the rule in a way which makes it mathematically accessible and which limits the parameter space. Thus, this study was guided by two objectives; (1) design a rule which is at an abstract level compatible with the biophysics of synaptic plasticity and (2) keep it simple to allow transfer into ANN design as well. We believe that the second aspect, which seems rather technical, is also important for the understanding of real synaptic plasticity, because at the moment there is still a wide gap between biological models of animal learning/memory and those for STDP and only a few attempts exist to model the one by means of the other (Sato and Yamaguchi, 2003; Melamed et al., 2004). Rules, like the one presented here, may offer the advantage of still being downward compatible with basic biophysical aspects while at the same time being upward compatible with models for learning and behavioral control (Porr and Wörgötter, 2003). We will start the discussion with a suggestion of how to use local plasticity rules in a functional context focusing on a semi-realistic neuronal implementation that we are currently pursuing (Tamosiunaite et al, in preparation) before trying to embed our approach into the literature.

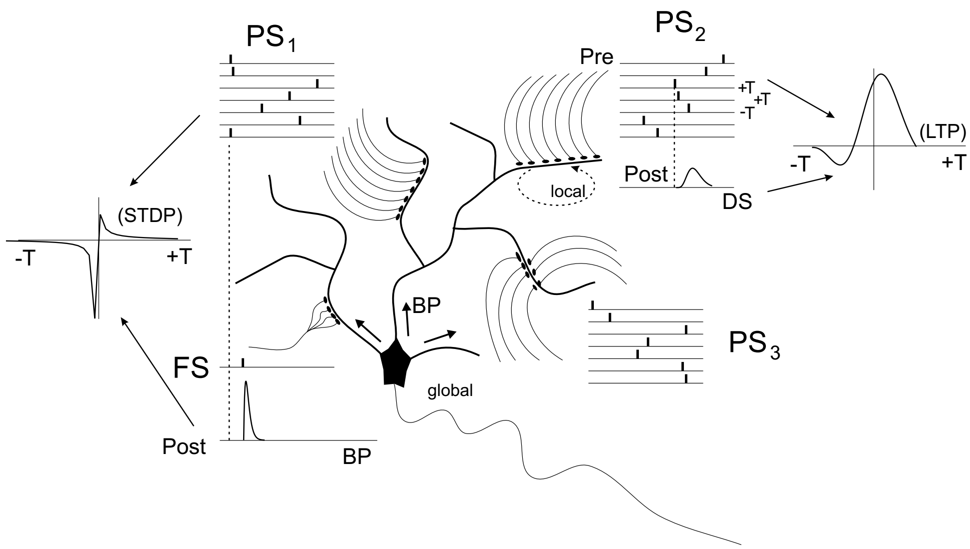

Figure 5: Implementation of different, parallel operating local learning mechanism at a neuron. For explanation see text.

4.2 Possible functional implications of local learning

Two very generic goals can be formulated for networks: 1) Networks need to select the "right" stimuli and 2) they should react early. Hence to the first appropriate stimulus. Fig. 5 shows a possible neuronal structure where local learning rules would be beneficial for achieving these two goals. Note, this example is clearly "engineered", but at this stage it is supposed to only show the potential of such mechanism, without treating details.

Let us assume that a neuron receives serveral (sensory) input-groups called $PS_{1,2,3}$. Early in development these inputs may well be weak but some of them are fairy synchronous, truly representing their associated stimulus. Since they are weak, they will not drive the soma, but one can assume that local processes between these synapses will take place. For example, the subgroup of synchronous inputs might elicit a small dendritic spike (DS) or at least a somewhat stronger, prololonged post-synaptic depolarization as compared to their non-synchronous peers. As shown in this study, such broad, long postsynaptic signals should essentially lead to hebbian learning (LTP). Hence all weights will grow, but predominantly those of the synchronous subgroup as long as $\pm T$ falls in the learning window. This may well happen independently at different parts of the dendrite selecting several subgroups. In this example one which responds early (PS_1), one in the middle (PS_2) and one late (PS_3). After some learning each PS subgroup might be able to drive the soma on its own, whereas the non-synchronous inputs remain behind. Hence local hebbian learnig has lead to input selection, which was the first goal specified above.

Let us furthermore assume that there is an independent, but strong input called FS which is able to drive (F=fire) the soma on its own. For the sake of simplicity the synaptic weight of this input is supposed to be constant.

All of the above introduiced stimuli might have the potential to be predictive of FS. That was the reason why they were called PS. However, the example is drawn in a way that only PS_1 comes before FS, hence PS_1 is the only "predictor" of FS, while $PS_{2,3}$ come too late.

Back-propagating spikes are often only elicited when the soma bursts (Kampa and Stuart, 2003a), i.e.; when more than one spike is elicited at the soma in a short temporal interval. This will in our example occur as soon as PS_1 and then FS fire the soma twice in rapid succession. A sharp BP spike will then travel retrogradely and interact with the PS clusters. Our study has shown that STDP is the consequence, where LTD occurs mainly for clusters '$PS_{2,3}$ and LTP for PS_1. Hence, after some learning only PS_1 (and FS) will still be able to drive the cell and it will respond earlier than in the beginning of the whole learning process. Hence, the system has achived the second goal, which can be interpreted as some kind of temporal sequence learning (Wörgötter and Porr, 2004).

In any true network implementation with its statistical properties this example operates in a much more complex way and we are currently investigating its properties. Here it shall suffice as an example of a possible network with interesting and useful local learning properties.

4.3 Downward compatibility: Limitations of our approach in comparison to biophysical models

Several models of intermediate biophysical realism exist which rely on a Ca^{2+} concentration dependent mechanisms involving NMDA-channels (Karmarkar and Buonomano, 2002; Senn et al., 2000; Castellani et al., 2001; Karmarkar et al., 2002; Shouval et al., 2002; Abarbanel et al., 2002, 2003). Essentially all of these models implement a Hebbian plasticity rule and a Ca^{2+} concentration dependent mechanism. Most of these models are faced with the problem that LTD should also occur for large positive values of T, where the Ca^{2+}-level will be as low as for negative T. Currently there is only one study which supports this (Nishiyama et al., 2000) and experimental evidence exist that the gradient of Ca^{2+} plays a major role, too (Mizuno et al., 2001). Thus, normally this effect is assumed to be undesirable and eliminated by including a temporal asymmetry around $T = 0$ in the plasticity rule (Karmarkar and Buonomano, 2002) and this argues for two different model mechanisms for LTP and LTD. Note, the split of terms observed in our study can to some degree implicitly accommodate also such an assumption by replacing the functions F and c_N as discussed in the results section above.

The central limitation of our model is that it is only at a rather abstract level capturing parts of the biophysical complexity of synaptic plasticity. The complexity of the different chemical reactions involved in generating STDP is indeed extremely high and only a few models have recently been described which try to capture some of its aspects in more detail. The kinetic model of (D'Alcantara et al., 2003) is based on the cascade of Ca^{2+}-induced chain reactions of calmodulin, CaMKII, calcineurin, phosphatase PP1, I-1 inhibitor, DARP-32 protein, protein kinase A (PKA) which leads to phoshorylation (increased activity, LTP) and dephosphorylation (decreased activity, LTD) of AMPA receptors. The model was tested by these authors with artificial step-like Ca^{2+} signals. In our hands, however, it did not reproduce the typical STDP curves (pilot study). Models of Holmes (2000) and Zhabotinsky (2000) investigate the interactions of calmodulin, CaMKII and calcineurin depending on the Ca^{2+} level but do not model LTP/LTD explicitly.

All the models discussed so far share the property that they cannot be treated analytically anymore and many times their behavior is heavily dependent on their (partly unknown) parameters. This can lead to problems in view of the fact that several aspects of STDP, particularly those concerning LTD, are either unknown or heavily debated. Our approach, on the other hand, simplifies this complexity to the level of a state-variable description using very few assumptions. This reduces the parameter space to a manageable level, makes the rule calculable, but carries the danger that some important aspects might have been missed.

However, basic compatibility with biophysics can in our situation be assessed by the predictions of the model. The three effects summarized above are at least semi-quantitative and should allow testing the model with some confidence.

4.4 Upward compatibility and comparison to more abstract STDP models

A central question that so far remains unanswered is: How can STDP be used to control learning? For example, some experimental and theoretical results suggest that STDP could be involved in temporal sequence learning (Yao and Dan, 2001; Mehta et al., 2002; Melamed et al., 2004) and in the control of place cell formation or memory encoding by theta phase precession in neurons of the Hippocampus (Gerstner and Abbott, 1997; Mehta et al., 2000; Sato and Yamaguchi, 2003).

Most older models for STDP *assume* a certain weight change curve which does not depend on the local properties of the cell (Gerstner et al., 1996; Abbott and Blum, 1996; Song et al., 2000; Rubin et al., 2001; Kempter et al., 2001). These models have mainly been used to model collective network properties, like weight and activity distributions (Song et al., 2000; Kempter et al., 2001). Others have been designed to generate map structures (Song and Abbott, 2001; Leibold et al., 2001; Kempter et al., 2001; Leibold and van Hemmen, 2002), direction selectivity (Buchs and Senn, 2002; Senn and Buchs, 2003) or temporal receptive fields (Leibold and van Hemmen, 2001). In addition, it was found that such networks can store patterns (Abbott and Blum, 1996; Seung, 1998; Abbott and Song, 1999; Fusi, 2002). Thus, so far the existing models do not make clear suggestions which would help addressing the problem of behavioral control by means of sequence learning.

In a recent study we were indeed able to show that essentially the same rule can be used to control temporal sequence learning in a robot (Porr and Wörgötter, 2003; Porr et al., 2003). However, the time-scales still do not match and "STDP-rule" had to be stretched to cover approximately $\pm 200ms$, which was the reaction time of sensor-motor coupling in the robot. This is due to the fact that we used only a single synapse between input and output, whereas in reality higher (non-reflexive) sensor-motor coupling needs normally many more stages. This requires linking neurons either in a chain like- (Abeles, 1991; Aviel et al., 2003) or recurrent loop architecture to cover the long temporal intervals between sensor and motor events. Chains of temporal low-pass filters like recently discussed by Abbott (2003) could be employed to this purpose. Rather intriguingly there is a recent result by Di Paolo. (2003) that shows that behavioral control in a robot can be improved using a network trained by STDP. In this study a genetic algorithm was used to select the best network from a set of networks all trained by STDP on a certain behavioral task. Genetic selection was performed over many generations. Finally a network was obtained, which was able to learn and control the behavioral task of positive and negative phototaxis in response to attractive and aversive stimuli. In this task the sensor motor loop would take sometimes more than 10 seconds. Unfortunately, due to the use of genetic programming, this study does not provide explicit knowledge about which properties are required in an STDP-network to successfully perform such sensor-motor coupling.

5 Appendix - Numerical Methods

Numerically, STDP curves were obtained by the following steps.

1. The recorded membrane traces (V_m) were scanned, semi-automatically digitized and convolved with the filter h (Eq. 3). F was numerically calculated from Eq. 2 and then correlated with the NMDA channel function c_N (Eq. 1. As required, correlation was performed in a temporally causal way by applying the shift operation to either F ($T \geq 0$) or to the NMDA channel function ($T < 0$). Thus,

$$\Delta\rho(T) = \mu \int_T^\infty F(t-T) c_N(t) dt, \quad T \geq 0 \tag{14}$$

$$\Delta\rho(T) = \mu \int_T^\infty F(t) c_N(t+T) dt, \quad T < 0 \tag{15}$$

numerically calculating these integrals. Note, the integration starts at T and not at zero, to avoid having to include a Heaviside function into the definition of c_N or F.

6 Acknowledgements

This work was supported by EPSRC and SHEFC. We wish to thank L. Smith, T. Mittmann and K. Gottmann for helpful discussions. Special thanks go to

Leo v. Hemmen who discussed the analytical solution with us in a slightly inconventional way between two lectures at the Göttingen Neurobiology Meeting at the lecture hall black board.

References

Abarbanel HDI, Huerta R, Rabinovich MI (2002) Dynamical model of long-term synaptic plasticity. *Proc. Natl. Acad. Sci. (USA)* 99:10132–10137.

Abarbanel HDI, Gibb L, Huerta R, Rabinovich MI (2003) Biophysical model of synaptic plasticity dynamics. *Biol Cybern* 89:214–226.

Abbott LF (2003) From synaptic dynamics to network function: Computational studies of plasticity. *Soc. Neurosci. Abstr. (Special Lecture)* 33:1.

Abbott LF, Blum KI (1996) Functional significance of long-term potentiation for sequence learning and prediction. *Cereb. Cortex* 6:406–416.

Abbott LS, Song S (1999) Temporal asymmetric Hebbian learning, spike timing and neuronal response variability In Kearns MS, Solla S, Cohn DA, editors, *Advances in Neural Information Processing Systems*, Vol. 11, pp. 69–75, Cambridge, MA. MIT Press.

Abeles M (1991) *Corticotronics: Neural Circuits of the Cerebral Cortex* Cambridge University Press.

Aviel Y, Mehring C, Abeles M, Horn D (2003) On embedding synfire chains in a balanced network. *Neural Comput* 15:1321–1340.

Bi GQ (2002) Spatiotemporal specificity of synaptic plasticity: cellular rules and mechanisms. *Biol. Cybern.* 87:319–332.

Bi GQ, Poo M (2001) Synaptic modification by correlated activity: Hebb's postulate revisited. *Annu. Rev. Neurosci.* 24:139–166.

Bliss TV, Gardner-Edwin AR (1973) Long-lasting potentiation of synaptic transmission in the dentate area of the unanaesthetized rabbit following stimulation of the perforant path. *J. Physiol. (Lond.)* 232:357–374.

Bliss TV, Lomo T (1970) Plasticity in a monosynaptic cortical pathway. *J. Physiol. (Lond.)* 207:61P.

Bliss TV, Lomo T (1973) Long-lasting potentiation of synaptic transmission in the dentate area of the anaesthetized rabbit following stimulation of the perforant path. *J. Physiol. (Lond.)* 232:331–356.

Buchs NJ, Senn W (2002) Spike-based synaptic plasticity and the emergence of direction selective simple cells: Simultation results. *J. Comput.Neurosci.* 13:167–186.

Castellani GC, Quinlan EM, Cooper LN, Shouval HZ (2001) A biophysical model of bidirectional synaptic plasticity: Dependence on AMPA and NMDA receptors. *Proc. Natl. Acad. Sci. (USA)* 98:12772–12777.

Chen H, Otmakhov N, Strack S, Colbran R, Lisman J (1999) Requirements for LTP induction by pairing in hippocampal CA1 pyramidal cell. *J. Neurophysiol.* 82:526–532.

D'Alcantara P, Schiffmann SN, Swillens S (2003) Bidirectional synaptic plasticity as a consequence of interdependent Ca2+-controlled phosphorylation and dephosphorylation pathways. *Eur J Neurosci* 17:2521–2528.

Debanne D, Gahwiler B, Thompson S (1998) Long-term synaptic plasticity between pairs of individual CA3 pyramidal cells in rat hippocampal slice cultures. *J. Physiol. (Lond.)* 507:237–247.

Di Paolo. EA (2003) Evolving spike-timing-dependent plasticity for single-trial learning in robots. *Philos Transact Ser A Math Phys Eng Sci* 361: 2299–2319 Evaluation Studies.

Feldmann D (2000) Timing-based LTP and LTD at vertical inputs to layer II/III pyramidal cells in rat barrel cortex. *Neuron* 27:45–46.

Froemke RC, Dan Y (2003) A dendritic gradient for the temporal window of spike-timing dependent plasticity in the visual cortex. *Soc. Neurosci. Abstr.* 33:123.5.

Fusi S (2002) Hebbian spike-driven synaptic plasticity for learning patterns of mean firing rates. *Biol. Cybern.* 87:459–470.

Gerstner W, Abbott LF (1997) Learning navigational maps through potentiation and modulation of hippocampal place cells. *J Comput Neurosci* 4:79–94.

Gerstner W, Kempter R, van Hemmen JL, Wagner H (1996) A neuronal learning rule for sub-millisecond temporal coding. *Nature* 383:76–78.

Golding NL, Jung H, Mickus T, Spruston N (1999) Dendritic calcium spike initiation and repolarization are controlled by distinct potassium channel subtypes in CA1 pyramidal neurons. *J. Neurosci.* 19:8789–8798.

Golding NL, Staff PN, Spurston N (2002) Dendritic spikes as a mechanism for cooperative long-term potentiation. *Nature* 418:326–331.

Hansel C, Artola A, Singer W (1997) Relation between dendritic Ca2+ levels and the polarity of synaptic long-term modifications in rat visual cortex neurons. *Eur J Neurosci* 9:2309–2322.

Häusser M, Mel B (2003) Dendrites: bug or feature? *Cur Opinion in Neurobiology* 13:372–383.

Häusser M, Spruston N, Stuart GJ (2000) Diversity and dynamics of dendritic signaling. *Science* 11:739–744.

Holmes WR (2000) Models of calmodulin trapping and CaM kinase II activation in a dendritic spine. *J Comput Neurosci* 8:65–85.

Hrabetova S, Serrano P, Blace N, Tse HW, Skifter DA, Jane DE, Monaghan DT, Sacktor TC (2000) Distinct NMDA receptor subpopulations contribute to long-term potentiation and long-term depression induction. *J Neurosci* 20:RC81.

Jahr CE, Stevens CF (1990) A quantitative description of NMDA receptor-channel kinetic behavior. *J.Neurosci.* 10:1830–1837.

Kampa BM, Stuart GJ (2003a) NMDA channel activiation during spike-timing dependent plasticity. *Soc. Neurosci. Abstr.* 33:257.5.

Kampa B, Stuart G (2003b) Dendritic mechanisms involved in spike-timing-dependent plasticity. *Proceedings of Sixth IBRO World Congress on Neuroscience, 2003, Prague, Czech Republic* p. 331.

Karmarkar UR, Buonomano DV (2002) A model of spike-timing dependent plasticity: One or two coincidence detectors? *J. Neurophysiol.* 88:507–513.

Karmarkar UR, Najarian MT, Buonomano DV (2002) Mechanisms and significance of spike-timing dependent plasticity. *Biol. Cybern.* 87:373–382.

Kempter R, Gerstner W, van Hemmen J. L. (2001) Intrinsic stabilization of output rates by spike-based Hebbian learning. *Neural Comp.* 13:2709–2741.

Kempter R, Leibold C, Wagner H, van Hemmen JL (2001) Formation of temporal-feature maps by axonal propagation of synaptic learning. *Proc. Natl. Acad. Sci. (USA)* 98:4166–4171.

Klopf AH (1986) A drive-reinforcement model of single neuron function In Denker JS, editor, *Neural networks for computing: AIP Conf. Proc.*, Vol. 151. New York: American Institute of Physics.

Koch C (1999) *Biophysics of Computation* Oxford University Press.

Koester HJ, Sakmann B (1998) Calcium dynamics in single spines during coincident pre- and postsynaptic activity depend on relative timing of back-propagating action potentials and subthreshold excitatory postsynaptic potentials. *Proc Natl Acad Sci U S A* 95:9596–9601.

Koester HJ, Sakmann B (2000) Calcium dynamics associated with action potentials in single nerve terminals of pyramidal cells in layer 2/3 of the young rat neocortex. *J Physiol* 529 Pt 3:625–646.

Kombian SB, Malenka RC (1994) Simultaneous LTP of non-NMDA- and LTD of NMDA-receptor-mediated responses in the nucleus accumbens. *Nature* 368:242–246.

Kosco B (1986) Differential Hebbian learning In Denker JS, editor, *Neural networks for computing: AIP Conference Proc. proceedings*, Vol. 151. New York: American Institute of Physics.

Kourrich S, Chapman CA (2003) NMDA receptor-dependent long-term synaptic depression in the entorhinal cortex in vitro. *J Neurophysiol* 89:2112–2119.

Kovalchuk Y, Eilers J, Lisman J, Konnerth A (2000) NMDA receptor-mediated subthreshold Ca^{2+}-signals in spines of hippocampal neurons. *J. Neurosci.* 20:1791–1799.

Larkum ME, Zhu JJ, Sakmann B (2001) Dendritic mechanisms underlying the coupling of the dendritic with the axonal action potential initiation zone of adult rat layer 5 pyramidal neurons. *J. Physiol. (Lond.)* 533:447–466.

Leibold C, Kempter R, van Hemmen JL (2001) Temporal map formation in the barn owl's brain. *Phys. Rev. Lett.* 87:248101–1–248101–4.

Leibold C, van Hemmen JL (2001) Temporal receptive fields, spikes, and Hebbian delay selection. *Neural Networks* 14:805–813.

Leibold C, van Hemmen JL (2002) Mapping time. *Biol. Cybern.* 87:428–439.

Linden DJ (1999) The return of the spike: Postsynaptic action potentials and the induction of LTP and LTD. *Neuron* 22:661–666.

Lisman J (1994) The CaM kinase II hypothesis for the storage of synaptic memory. *Trends Neurosci.* 17:406–412.

Magee JC, Johnston D (1997) A synaptically controlled, associative signal for Hebbian plasticity in hippocampal neurons. *Science* 275:209–213.

Malenka RC, Nicoll RA (1999) Long-term potentiation-a decade of progress? *Science* 285:1870–1874.

Markram H, Lübke J, Frotscher M, Sakmann B (1997) Regulation of synaptic efficacy by coincidence of postsynaptic APs and EPSPs. *Science* 275:213–215.

Mehta MR, Lee AK, Wilson MA (2002) Role of experience and oscillations in transforming a rate code into a temporal code. *Nature* 417:741–746.

Mehta MR, Quirk MC, Wilson MA (2000) Experience-dependent asymmetric shape of hippocampal receptive fields. *Neuron* 25:707–715.

Mel B (1994) Information processing in dendritic trees. *Neural Computation* 6:1031–1085.

Melamed O, Gerstner W, Maass W, Tsodyks M, Markram H (2004) Coding and learning of behavioral sequences. *Trends Neurosci* 27:11–14.

Mizuno T, Kanazawa I, Sakurai M (2001) Differential induction of LTP and LTD is not determined solely by instantaneous calcium concentration: an essential involvement of a temporal factor. *Eur J Neurosci* 14:701–708.

Monyer H, Burnashev N, Laurie D, Sakmann B, H. SP (1994) Developmental switch in the expression of NMDA receptors occurs in vivo and in vitro. *Neuron* 12:529–540.

Nishiyama M, Hong K, Mikoshiba K, Poo M, Kato K (2000) Calcium stores regulate the polarity and input specificity of synaptic modification. *Nature* 408:584–588.

Normann C, Peckys D, Schulze CH, Walden J, Jonas P, Bischofberger J (2000) Associative long-term depression in the hippocampus is dependent on postsynaptic N-type Ca2+ channels. *J Neurosci* 20:8290–8297.

Oliet SH, Malenka RC, Nicoll RA (1997) Two distinct forms of long-term depression coexist in CA1 hippocampal pyramidal cells. *Neuron* 18: 969–982.

Otmakhov N, Griffith L, Lisman J (1997) Postsynaptic inhibitors of calcium/calmodulin-dependent protein kinase type II block induction but not maintenance of pairing-induced long-term potentiation. *J. Neurosci.* 17:5357–5367.

Poirazi P, Brannon T, Mel B (2003) Arithmetic of subthreshold synaptic summation in a model CA1 pyramidal cell. *Neuron* 37:977–987.

Porr B, von Ferber C, Wörgötter F (2003) ISO-learning approximates a solution to the inverse-controller problem in an unsupervised behavioral paradigm. *Neural Comp.* 15:865–884.

Porr B, Wörgötter F (2003) Isotropic sequence order learning. *Neural Comp.* 15:831–864.

Rao RPN, Sejnowski TJ (2001) Spike-timing-dependent Hebbian plasticity as temporal difference learning. *Neural Comp.* 13:2221–2237.

Roberts PD (1999) Temporally asymmetric learning rules: I. Differential Hebbian learning. *J. Comput. Neurosci.* 7:235–246.

Rubin J, Lee DD, Sompolinsky H (2001) Equilibrium properties of temporally asymmetric Hebbian plasticity. *Phys. Rev. Lett.* 86:364–367.

Sabatini BL, Oertner TG, Svoboda K (2002) The life cycle of Ca(2+) ions in dendritic spines. *Neuron* 33:439–452.

Sato N, Yamaguchi Y (2003) Memory encoding by theta phase precession in the hippocampal network. *Neural Computation* 15:2379–2397.

Saudargiene A, Porr B, Wörgötter F (2004) How the shape of pre- and postsynaptic signals can influence STDP: a biophysical model. *Neural Comp.* 16:595–626.

Sawtell NB, Huber KM, Roder JC, Bear MF (1999) Induction of NMDA receptor-dependent long-term depression in visual cortex does not require metabotropic glutamate receptors. *J Neurophysiol* 82:3594–3597.

Schiller J, Major G, Koester HJ, Schiller Y (2000) NMDA spikes in basal dendrites of cortical pyramidal neurons. *Nature* 11: 285–289.

Senn W, Buchs NJ (2003) Spike-based synaptic plasticity and the emergence of direction selective simple cells: mathematical analysis. *J. Comput. Neurosci.* 14:119–138.

Senn W, Markram H, Tsodyks M (2000) An algorithm for modifying neurotransmitter release probability based on pre-and postsynaptic spike timing. *Neural Comp.* 13:35–67.

Seung HS (1998) Learning continous attractors in recurrent networks In Kearns M, Jordan M, Solla S, editors, *Advances in Neural Information Processing Systems*, pp. 654–660, Cambridge, MA. MIT Press.

Shouval HZ, Bear MF, Cooper LN (2002) A unified model of NMDA receptor-dependent bidirectional synaptic plasticity. *Proc. Natl. Acad. Sci. (USA)* 99:10831–10836.

Sjöström PJ, Turrigiano GG, Nelson SB (2001) Rate, timing, and cooperativity jointly determine cortical synaptic plasticity. *Neuron* 32:1149–1164.

Song S, Abbott LF (2001) Cortical remapping through spike timing-dependent plasticity. *Neuron* 32:1–20.

Song S, Miller KD, Abbott LF (2000) Competitive Hebbian Learning through spike-timing-dependent synaptic plasticity. *Nature Neurosci.* 3:919–926.

Stuart G, Spruston N (1998) Determinants of voltage attenuation in neocortical pyramidal neuron dendrites. *J Neuroscience* 18:3501–3510.

Sutton R, Barto A (1981) Towards a modern theory of adaptive networks: Expectation and prediction. *Psychol. Review* 88:135–170.

Wessel R, Kristan WBJ, Kleinfeld D (1999) Dendritic Ca(2+)-activated K(+) conductances regulate electrical signal propagation in an invertebrate neuron. *J Neurosci* 19:8319–8326.

Williams K, Russell S, Shen Y, Molinoff P (1993) Developmental switch in the expression of NMDA receptors occurs in vivo and in vitro. *Neuron* 10:267–278.

Wörgötter F, Porr B (2004) Temporal sequence learning, prediction and control: A review of different models and their relation to biological mechanisms. *Neural Comp.*: in press.

Xie X, Seung S (2000) Spike-based learning rules and stabilization of persistant neural activity In Solla SA, Leen TK, Müller KR, editors, *Advances in Neural Information Processing Systems*, Vol. 12, pp. 199–208, Cambridge, MA. MIT Press.

Yang SN, Tang YG, Zucker RS (1999) Selective induction of LTP and LTD by postsynaptic [Ca2+]i elevation. *J Neurophysiol* 81:781–787.

Yao H, Dan Y (2001) Stimulus timing-dependent plasticity in cortical processing of orientation. *Neuron* 32:315–323.

Zhabotinsky AM (2000) Bistability in the Ca(2+)/calmodulin-dependent protein kinase-phosphatase system. *Biophys J* 79:2211–2221.